



Roles of marine ice, rheology, and fracture in the flow and stability of the Brunt/Stancomb-Wills Ice Shelf

A. Khazendar,¹ E. Rignot,^{1,2} and E. Larour¹

Received 6 August 2008; revised 18 June 2009; accepted 1 July 2009; published 27 October 2009.

[1] Marine ice, sometimes as part of an ice mélange, significantly affects ice shelf flow and ice fracture. The highly heterogeneous structure of the Brunt/Stancomb-Wills Ice Shelf (BSW) system in the east Weddell Sea offers a rare setting for uncovering the difference in rheology between meteoric and marine ice. Here, we use data assimilation to infer the rheology of the Brunt/Stancomb-Wills Ice Shelf by an inverse control method that combines interferometric synthetic aperture radar measurements with numerical modeling. We then apply the inferred rheology to support the hypothesis attributing the observed 1970s ice shelf flow acceleration to a change in the stiffness of the ice mélange area connecting Brunt proper with Stancomb-Wills and to examine the consequences of frontal rift propagation. We conclude that while the Brunt/Stancomb-Wills system is currently not susceptible to extreme fragmentation similar to that of the Larsen B Ice Shelf in 2002, our inverse and forward modeling results emphasize its vulnerability to destabilization by relatively rapid changes in the ice mélange properties, resulting from the interaction of its marine ice component with ocean water, or by the further propagation of a frontal rift.

Citation: Khazendar, A., E. Rignot, and E. Larour (2009), Roles of marine ice, rheology, and fracture in the flow and stability of the Brunt/Stancomb-Wills Ice Shelf, *J. Geophys. Res.*, *114*, F04007, doi:10.1029/2008JF001124.

1. Introduction

[2] The disintegration of ice shelves along the Antarctic Peninsula over the past two decades demonstrated unambiguously the link between the removal of ice shelves and the acceleration of their tributary glaciers [Rignot *et al.*, 2004; Scambos *et al.*, 2004]. This increased discharge of continental ice to the ocean contributes directly to global sea level rise and emphasizes the need for improved understanding of ice shelf evolution in a warming climate.

[3] Marine ice is an important factor in ice shelf stability, both in the manner that its presence affects ice shelf flow and mechanical properties, and in its interaction with fracture features. Several Antarctic ice shelves have been shown to be composed of marine ice, several tens of meters in thickness, at many locations [e.g., Morgan, 1972; Oerter *et al.*, 1994; Fricker *et al.*, 2001]. Distinct from meteoric or sea ice, marine ice forms when frazil ice crystals accumulate at the base of an ice shelf as part of the thermohaline circulation in the underlying cavity [Jenkins and Bombosch, 1995] and subsequently consolidate into layers, the lower of which can be highly porous [Engelhardt and Determann, 1987; Craven *et al.*, 2005]. Fracture, itself a critical aspect of ice shelf stability, is often affected by marine ice, which

can fill rifts and bottom crevasses [Khazendar *et al.*, 2001; Khazendar and Jenkins, 2003]. The heterogeneous material composed of marine ice, sea ice, ice shelf debris and firn is referred to as an ice mélange. Several investigators [Ardus, 1965; Stephenson and Zwally, 1989; Doake and Vaughan, 1991] have suggested that the ice mélange acts as a binding material that slows or halts rift enlargement or, on a much larger scale, holds extensive segments of an ice shelf together. Rignot and MacAyeal [1998] and MacAyeal *et al.* [1998] showed that the ice mélange tends to deform coherently in reaction to ice shelf flow and that it has sufficient mechanical strength and integrity to bind large tabular ice shelf fragments to the coast, and Larour *et al.* [2004] found that ice mélange in rifts exerts a major influence on their propagation.

[4] A prominent feature of the system in the eastern sector of the Weddell Sea composed of the Brunt Ice shelf, where Halley Research Station has been located since 1956, and the Stancomb-Wills Ice Tongue, is that the two floating glaciers are connected by a large, visible expanse of ice mélange (Figure 1). This mélange comprises 20–30% of the 29,000 km² surface area of the system [Hulbe *et al.*, 2005]. Another smaller area of ice mélange separates the north-eastern edge of Stancomb-Wills from Lyddan Island. The ice mélange thickness, which exceeds 100 m in many locations, cannot be explained by firn, ice shelf debris and sea ice alone and, hence, must contain a significant portion of marine ice. This is supported by ocean circulation modeling of the east Weddell Sea [Thoma *et al.*, 2006], which predicts that freezing at the ice-ocean interface under the ice shelf takes place at the grounding lines upstream

¹Jet Propulsion Laboratory, California Institute of Technology, Pasadena, California, USA.

²Earth System Science, University of California, Irvine, California, USA.

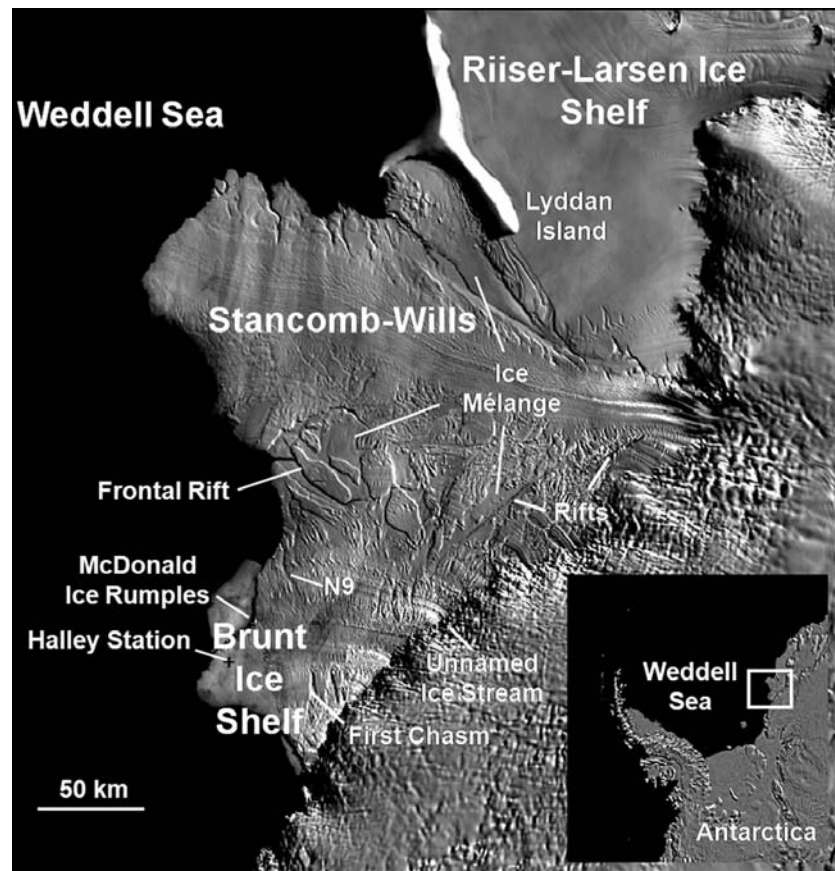


Figure 1. Morphological and structural features of the Brunt/Stancomb-Wills system. The background radar backscatter image is from *Haran et al.* [2005]. The designations of rifts N9 and First Chasm are from a document by the *British Antarctic Survey* [2005].

from the two ice *mélange* areas. Satellite interferometry [Rignot, 2002] and forward numerical modeling [Hulbe et al., 2005; Humbert and Pritchard, 2006] have now clearly established the strong dynamic connection and interaction between the ice *mélange* area and surrounding meteoric ice of Stancomb-Wills and Brunt proper. Several other Antarctic ice shelves are known to be composed of meteoric ice sections that are held together by ice *mélange* bodies, including Larsen D, Shackleton and West ice shelves, and probably many others where the presence of ice *mélange* is not yet as readily discernable.

[5] In this paper, we seek to test the hypothesis that by applying data assimilation methods we can detect the difference in stiffness, as expressed in the values of the flow parameter, between the two types of ice because of the different temperature regimes and compositions. The flow parameter is the proportionality coefficient between stress and strain in Glen's flow law, which depends mainly on ice temperature, fabric, impurity and water content [Paterson, 1994] and can be written as

$$\sigma' = B\dot{\epsilon}/e_{II}^{(n-1)/n}$$

where σ' is the deviatoric stress tensor, $\dot{\epsilon}$ is the strain rate tensor, e_{II} is the second invariant of the strain rate tensor, n is the power flow law exponent, and B is the flow parameter.

[6] Constraining the rheological properties of the ice is fundamental for accurate ice shelf forward modeling. The

increasing availability of satellite-borne interferometric synthetic aperture radar (InSAR) observations has made possible the fruitful application of inverse modeling techniques to infer the rheological properties of ice sheets. Data assimilation on ice shelf rheology has been thus far applied to estimate the viscosity of the Ross [Rommelaere and MacAyeal, 1997], the flow parameter of Ronne [Larour et al., 2005], and that of Larsen B [Vieli et al., 2006, 2007; Khazendar et al., 2007] ice shelves.

[7] We then apply forward modeling using the inferred rheology field to examine the flow of the ice shelf, in particular its hitherto unexplained acceleration during the 1970s, and the influence of possible variations in the stiffness of the ice *mélange* areas. We then test the response of the flow field to a probable enlargement of an already existing frontal rift. These simulations, and the indications from the inferred rheology concerning the stiffness of the ice shelf and the role of marine ice in filling fracture, leads us to a discussion of the present state of stability of the BSW system and its possible evolution.

2. Input Observations and Model

[8] The ice shelf velocity field (Figure 2) is mapped by applying a speckle tracking technique to RADARSAT-1 data acquired in September–November 2000, with gaps filled using data acquired in 1997 and adjusted for small

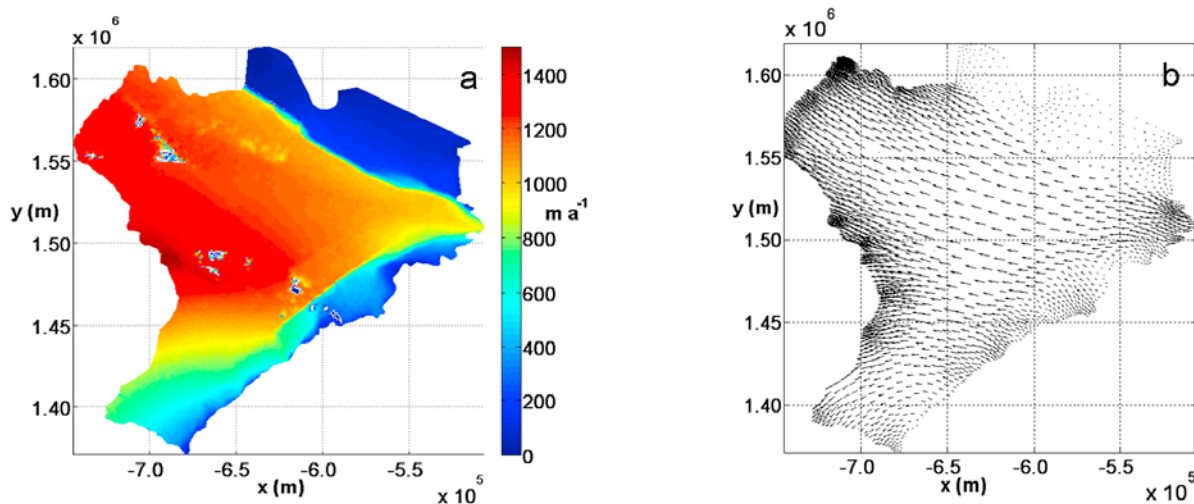


Figure 2. (a) The speed and (b) velocity vector fields of the Brunt/Stancomb-Wills system based on RADARSAT-1 observations made in 1997 and 2000. The patches are areas where the velocity could not be obtained. The velocity field does not show any discontinuity between Stancomb-Wills and the central ice mélange area, thus demonstrating their kinematic unity despite their constituent heterogeneity. On the other hand, notice the abrupt change in velocity magnitude along rifts and strong shearing zones, including the frontal rift, north of which speed is abruptly higher.

biases, assuming no temporal variability in the flow between the two years. Areas known to be stagnant such as ice rises and islands defined an absolute reference frame for the velocities. The accuracy of the measurements is about 10 m a^{-1} at 50 m posting, with tidal effects probably contributing to a larger error in ground range. Thus, given a repeat cycle of 24 days and an incidence angle of 35° , the error in range is approximately 20 m a^{-1} . Obtaining the speeds averaged over the 24-day repeat cycle ensures that errors due to tidal movements [Doake *et al.*, 2002] are insignificant. The 1997 data were acquired during the first Antarctic Mapping Mission (AMM-1) in the fall of 1997, while the 2000 data were acquired during the second Antarctic Mapping Mission (AMM-2) in the fall of 2000. Figure 2 shows that the flow of the Stancomb-Wills Ice Tongue dominates the measured velocity field, and is delimited on its northeastern and southern flanks by sharp velocity gradients. The highest measured speeds of around 1500 m a^{-1} are attained, not at the central and most advanced part of the ice tongue front, but at its edge where it meets the ice mélange area, thus confirming the findings of Hulbe *et al.* [2005] that the ice mélange area connects the two main parts of the BSW system and shifts the kinematic center of the system southward and westward.

[9] The grounding line is inferred from ERS-1/2 data (from 1996 for fast flow areas) and RADARSAT-1 (from 2000 for slower moving areas) using double difference interferometry with a precision of 100 m . Ice shelf elevations (Figure 3) are taken from the GLAS/ICE Sat laser altimeter digital elevation model of Antarctica [DiMarzio *et al.*, 2007] generated from observations made between 2003 and 2005. Ice shelf thickness is calculated from these elevations assuming hydrostatic equilibrium and adjusting for the presence of firm. No detailed firm density profiles could be found for the BSW system, we therefore base our firm estimates on van den Broeke [2006, 2008]. These studies, which combine

regional climate and firm densification models, predict that the 830 kg m^{-3} firm density depth to be $55\text{--}65 \text{ m}$ for the BSW area. The models, however, do not include surface melting, observed to occur on average during $8\text{--}30$ days annually [Liu *et al.*, 2006], which would increase firm density. Furthermore, the strong negative firm depth trend of the BSW area simulated by Helsen *et al.* [2008] and attributed mainly to decreasing accumulation also suggests higher firm density. We therefore adjust ice shelf thickness by assuming a uniform

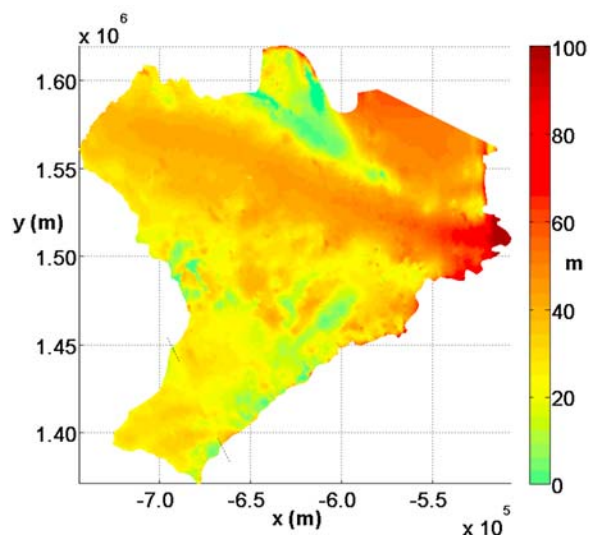


Figure 3. Ice surface elevation of Brunt/Stancomb-Wills from the GLAS/ICESat laser altimetry DEM [DiMarzio *et al.*, 2007]. The ice mélange areas indicated in Figure 1 are revealed here to be low lying and relatively flat. The two dashed lines in the Brunt Ice Shelf area mark the ends of the fault that seems to extend from the grounding line to the front, joining N9 with the big rift to the southeast of First Chasm.

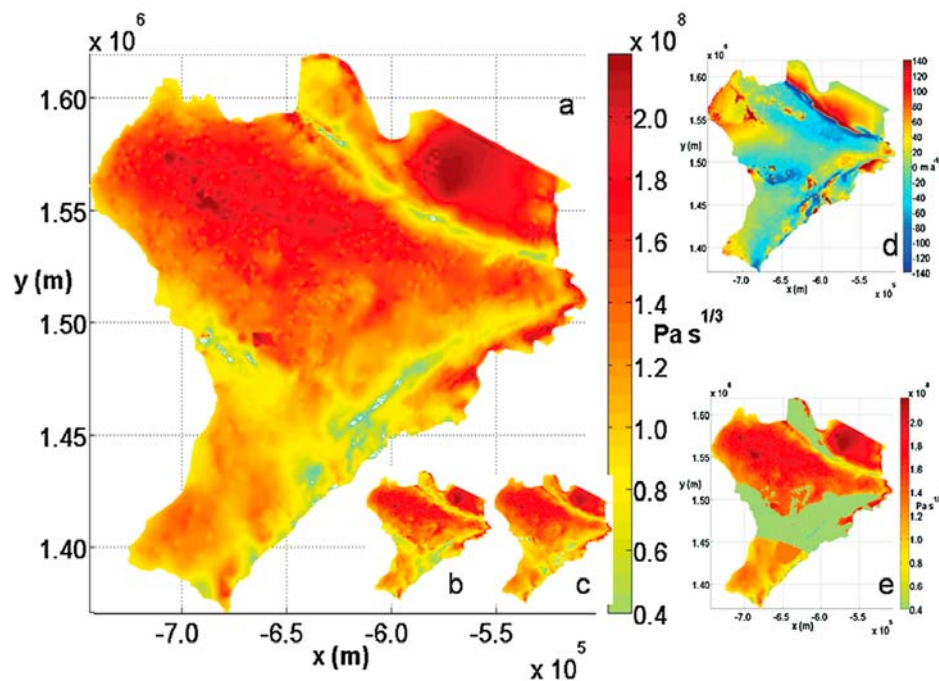


Figure 4. (a) The inferred flow parameter distribution for $B_0 = 0.8 \times 10^8 \text{ Pa s}^{1/3}$ after 60 iterations. Confidence in this result is further enhanced by the fact that model outputs for B_0 values in a range extending from (b) $0.7 \times 10^8 \text{ Pa s}^{1/3}$ to (c) $1.0 \times 10^8 \text{ Pa s}^{1/3}$ converge reasonably well. (d) The discrepancy obtained by subtracting the observed speeds from speeds simulated using the flow parameter field in Figure 4a. (e) Rheology field used in the simulations of the 1970s BSW system acceleration, modified from that of Figure 4a by reducing the flow parameter value of the mélange areas to $0.4 \times 10^8 \text{ Pa s}^{1/3}$ and increasing that of fracture zone in the unnamed ice stream to $1.3 \times 10^8 \text{ Pa s}^{1/3}$.

firm layer of 65 m, at the density of 830 kg m^{-3} . In this approximation, setting firm depth at the higher end of the 55–65 m simulated by *van den Broeke* [2006, 2008] should compensate for the lower density higher in the firm column. The density of ice mélange areas should be close to that of the rest of the ice shelf as fully consolidated marine ice, the main component there in addition to firm and ice shelf fragments, has the same density as meteoric ice within measurement error [*Oerter et al.*, 1994].

[10] The data assimilation process seeks a depth-averaged spatial distribution of the flow parameter that, when substituted into a finite element forward model, minimizes the difference between model output and observations. Analysis by *Thomas* [1973a] demonstrated the applicability of Glen’s flow law to the Brunt Ice Shelf, including ice mélange areas, and we here use the *MacAyeal* [1989] ice shelf flow model, with InSAR velocity observations imposed at the grounding line. The inverse control method is based on the work by *MacAyeal* [1992], with the modifications of having seawater pressure as the boundary condition at the ice front, and inverting directly for the flow parameter [*Larour et al.*, 2004, 2005]. One advantage of the inverse modeling we implement here is that no special treatment is required for the ice shelf basal friction that occurs at the McDonald Ice Rumples east of Halley Station (Figure 1) as would be done in a forward modeling study by prescribing a friction parameter [*Hulbe et al.*, 2005]. The presence of this area of grounded ice is already reflected in the measured velocity field and should accordingly imprint the inferred rheology

distribution. The model is initiated with an approximate uniform value of the stiffness, B_0 , producing a first estimate of the misfit between modeled and observed velocities. The process is repeated with modified flow parameter values at least until the misfit variation falls below 1%.

[11] We define a model domain roughly similar to that of *Hulbe et al.* [2005]. Observations and model results are shown in polar stereographic coordinates. Our mesh contains about 21,000 elements, with element sizes varying between 500 and 3000 m for better representation of ice shelf geometry and features.

3. Results

[12] The inferred spatial distribution of the vertically integrated flow parameter, shown in Figure 4, exhibits excellent correspondence with the structural and morphological features visible in the backscatter radar image of Figure 1. Thus, the colder ice outflow of the Stancomb-Wills Ice Stream can be easily traced from the grounding line to the front by its relatively higher stiffness. At the northeastern flank of Stancomb-Wills, the highly crevassed narrow zone of strong shearing is faithfully reproduced as a strip of much weaker ice separating it from the area of stiff ice in the part of the Riiser-Larsen Ice Shelf included in our model domain. The other main area of marked fracture, south of Stancomb-Wills and composed of at least two linear rifts running in parallel to the grounding line (Figure 1), is also accurately marked in the inferred rheology (Figure 4).

Also well represented are the other two zones of pronounced fracture, one around the rift in the mélange area at the ice shelf front (Figure 1), and the other composed of a series of transverse crevasses and rifts open in the section of the unnamed ice stream (Figure 1) nearer to the grounding line.

[13] Using the inferred rheology to run the ice shelf flow model and subtracting the observed velocity magnitude from its output gives the residual shown in Figure 4d. Modeled speeds deviate by less than $\pm 50 \text{ m a}^{-1}$ at most locations, in excellent agreement with observations. The highest residual is found on both sides of the strong shearing strip at the northeastern flank of Stancomb-Wills. Our data assimilation successfully simulated the weakness of the ice along this boundary, but the decoupling is probably incomplete. Hence, the almost stagnant ice of Riiser-Larsen still feels the pull of the much faster Stancomb-Wills, which results in our forward model, using the inferred rheology, overestimating its speed. The opposite effect takes place on the Stancomb-Wills side.

4. Discussion

4.1. Rheological Difference of Marine and Meteoric Ice

[14] The results presented in Figure 4 show that there is a clear and consistent difference in the stiffness of meteoric and marine ice areas. Riiser-Larsen Ice Shelf, Stancomb-Wills and parts of Brunt Ice Shelf proper have flow law parameter values mostly in the range of 1.5×10^8 to $1.9 \times 10^8 \text{ Pa s}^{1/3}$ (475 to 601 kPa $\text{a}^{1/3}$). On the other hand, the main ice mélange area, between Brunt proper and Stancomb-Wills is demarcated in the flow parameter field (Figure 4) from the stiffer Stancomb-Wills by a clear jump along a line that follows remarkably well the morphological features of Figure 1. It has the lower flow parameter value range of 1.0×10^8 to $1.3 \times 10^8 \text{ Pa s}^{1/3}$ (317 to 411 kPa $\text{a}^{1/3}$). A similar range of values was found for the smaller mélange area between the northeastern flank of Stancomb-Wills and Lyddan Island, which further enhances confidence in our results by demonstrating the consistency of the inferred difference in stiffness between meteoric and mélange areas including marine ice.

[15] The distinct rheology of the two types of ice in the current setting is largely due to their different thermodynamic regimes. According to the field and experimental data sets compiled by Paterson [1994], the meteoric ice flow parameter range inferred here corresponds to temperatures between -21°C and -15°C , while that of the ice mélange to -11°C to -7°C . Because marine ice forms in the ocean, it is possible to constrain its approximate temperature from the surface and bottom temperatures of the ice shelf, making the assumption that there was little thermal exchange with meteoric ice. The temperature at the interface between the bottom of the ice shelf and ocean is close to -2°C [Fofonoff and Millard, 1983], the freezing temperature of seawater. An indication of the surface temperature of the ice shelf is given by the long-term mean temperature of -18.5°C measured at Halley Station for the period 1957–1995 [van den Broeke, 2000]. These two boundary temperatures therefore reasonably bracket the temperature range implied by our rheology results for the ice mélange, and the agreement further demonstrates the reliability of the flow parameter values we inferred for these areas.

[16] Meteoric ice, on the other hand, is mostly advected from the interior of the continent and is therefore certain to be colder than marine ice. We constrain its temperatures by the measurements of Renfrew and Anderson [2002] from a weather station on Coats Land, 155 km to the South of Halley Station in the interior of the continent, which records mean seasonal surface temperatures varying between -31°C and -15°C . Furthermore, thermodynamic modeling by Hulbe et al. [2005] suggests that the bulk of the thickness of Stancomb-Wills at its grounding line is between -25°C and -15°C , again in good agreement with our results.

[17] While we could demonstrate the role of temperature in the inferred stiffness differences, the distinct crystallographic structure and salinity and impurity contents of marine ice [Moore et al., 1994; Eicken et al., 1994; Khazendar et al., 2001] may play a part, but which cannot be discerned in the present study. Rist et al. [2002] studied the mechanical fracture behavior of both meteoric and marine ice under certain conditions, finding that fracture toughness related to crevasse propagation is slightly higher for marine ice, but such processes are also not included in our model.

[18] Finally, in the zones of intense fracture and shearing the flow parameter is mostly between 0.2×10^8 and $0.6 \times 10^8 \text{ Pa s}^{1/3}$ (63 to 190 kPa $\text{a}^{1/3}$). The lower part of this range is below what would be expected for ice at 0°C , measured in the laboratory and the field to be between 0.4×10^8 to $0.7 \times 10^8 \text{ Pa s}^{1/3}$ (135 to 228 kPa $\text{a}^{1/3}$) [Paterson, 1994]. Investigators of ice shelf processes have already drawn attention to ice conditions that would no longer conform to some of the underlying assumptions of Glen's flow law of homogeneity, continuity and isotropy [Rommelaere and MacAyeal, 1997]. Hence, these low flow parameter values are not only a manifestation of the intrinsic properties of the ice, but also of the presence of fracture, which translates as higher strain rate and correspondingly lower inferred stiffness, as the forward model, which is based on the assumptions of continuum mechanics, attempts to accommodate the observed velocities of fractured areas of the domain.

[19] Along the ice shelf front of Brunt proper, the highest flow parameter values are around the McDonald Ice Rumples, where the resistance that ice shelf flow encounters at this ice rise manifests itself as stiffer ice.

4.2. Simulation of the 1970s Ice Shelf Acceleration

[20] Insights into the possible role of marine ice are gained by examining the causes of the BSW acceleration during the 1970s, which occurred irregularly over the period from 1972 to 1982. Simmons and Rouse [1984] and Simmons [1986] calculated that the westward speed of Halley Station increased from $431 \pm 22 \text{ m a}^{-1}$ for the period 1968–1971 to $740 \pm 9 \text{ m a}^{-1}$ for the period 1972–1982. The former authors thought that it was unclear whether a calving event in 1971–1973 would result in the observed sustained increase in velocity, leaving a generalized acceleration of the system, especially that of Stancomb-Wills, as a plausible explanation [Simmons and Rouse, 1984; Doake, 2000; Thomas, 2007]. Indeed, Orheim [1986] measured velocity magnitudes at the front of Stancomb-Wills of up to 4000 m a^{-1} (compared with about 1500 m a^{-1} measured here) for the period 1973 to 1977, and Lange and Kohnen [1985] reported comparably high frontal velocities. These observations establish that the acceleration at Halley

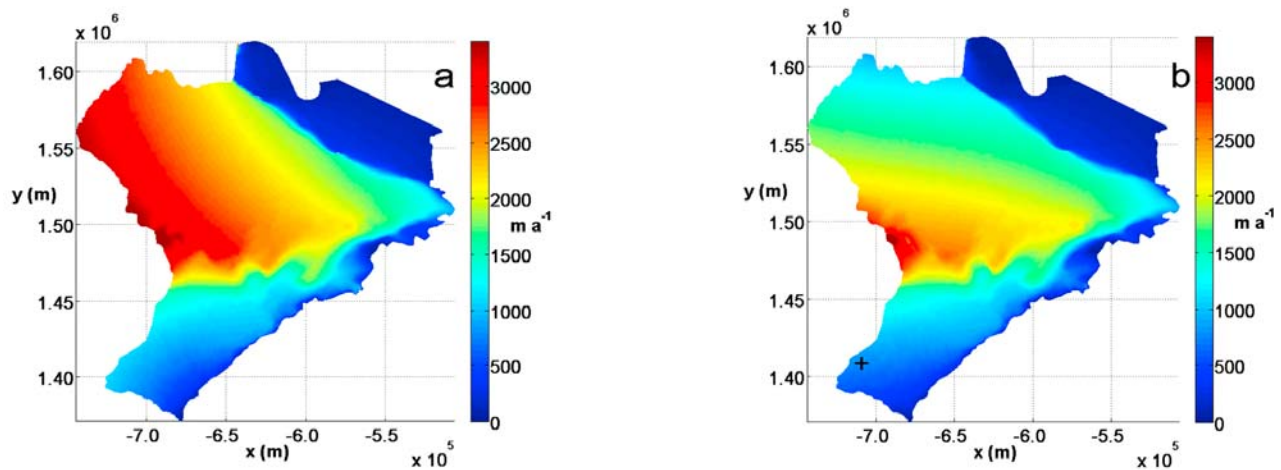


Figure 5. (a) The speed field resulting from the forward model run employing the rheology in Figure 4e. Speed reaches 3800 m a^{-1} at the front of Stancomb-Wills. (b) The corresponding easting speed component showing the speed at the 1968 location of Halley Station (obtained from *Simmons and Rouse* [1984]), which is marked by a cross, at 787 m a^{-1} .

Station was part of wider changes that affected the whole BSW system at that time. The changing interaction with the McDonald Ice Rumples following the calving event is an insufficient explanation as its effect would have been local. Further clues to the extent of these changes can be found in the backscatter radar image, which shows that the unnamed ice stream (Figure 1) has changed its flow direction producing the series of transverse rifts and crevasses that appear as a pronounced weakness in the inferred rheology. More salient still is the fault, revealed by closer examination of the ice surface elevation map (Figure 3), extending from the grounding line to the front, along which the ice shelf was clearly broken resulting in the displacement of one side relative to the other. This shows that the two fracture features, N9 (Figure 1) and the big rift to the southeast of First Chasm, are actually part of the same fault. *Hayes* [2005] had speculated that fractures at the front and near the grounding line of Brunt could join.

[21] Here we simulate the accelerated flow of the BSW system using velocity observations from the 1970s at two different locations of Halley and the front of Stancomb-Wills [*Simmons and Rouse*, 1984; *Simmons*, 1986; *Orheim*, 1986; *Lange and Kohnen*, 1985] to better constrain, and more conclusively compare with, the output of our experiments. An initial test, using the inferred rheology (Figure 4a), excluded acceleration of the outflow of the Stancomb-Wills Ice Stream into the ice shelf as the sole explanation of the observed changes during the 1970s, because replicating these observations required an unrealistic ninefold increase in the outflow velocity at the grounding line. We therefore examine the possibility, which was noted by *Simmons and Rouse* [1984] and *Doake* [2000], that these changes occurred as a result of modifications in the properties of the ice mélange areas. Furthermore, these occurrences could be cyclical, as suggested by recent measurements indicating that the ice shelf at Halley has been decelerating from about 750 m a^{-1} in 1999 to about 530 m a^{-1} in 2006 [*British Antarctic Survey*, 2007].

[22] We hypothesize that the BSW system accelerated because the ice mélange area weakened during the 1970s.

This could have taken place as part of the notable changes in the eastern Weddell Sea at the time. Thus, the most extensive polynya on record formed in that region between 1974 and 1976 [e.g., *Carsey*, 1980], probably as a result of deep oceanic convection [*Gordon*, 1982], or changes in the interaction of large-scale circulation with seabed topography [*Holland*, 2001] bringing warmer deep water closer to the surface. *Robertson et al.* [2002], on the other hand, discuss changes in the inflow of water masses into the eastern Weddell Sea in the early 1970s. Furthermore, theoretical work [*Beckmann and Timmermann*, 2001] identifies a temperature anomaly with decadal periodicity that travels counterclockwise along the Antarctic coast. The continental shelf off Brunt and Stancomb-Wills is relatively narrow, thus making the cavity beneath the ice shelf more accessible to warmer ocean water that could have weakened the layers of marine ice in the lower parts of the ice mélange areas. Fieldwork shows that fully consolidated bodies of marine ice can be underlain by layers of tens of meters of marine ice exhibiting a highly porous structure that makes it permeable to ocean water while still possessing mechanical integrity [*Engelhardt and Determann*, 1987; *Craven et al.*, 2004, 2005]. The latter two studies of a 480-m borehole in the Amery Ice Shelf revealed that the lower 200 m were composed of marine ice, the bottom 100 m of which were so porous that the brine channels and pores were hydraulically connected to the ocean.

[23] We simulate weaker ice mélange by imposing on its two main areas (Figure 4e) a flow parameter value of $0.4 \times 10^8 \text{ Pa s}^{1/3}$, which is the lowest value measured for ice in laboratory and field work [*Paterson*, 1994], and is the middle point in our inferred range for the zones of weakest ice. Running the forward model with this rheology distribution produces speeds that are in reasonable agreement with those observed at the two reference points. Thus, the velocity magnitude at the front of Stancomb-Wills increases to 3800 m a^{-1} (Figure 5a), consistent with *Orheim* [1986], while the easting speed at the 1968 location of Halley Station reaches 836 m a^{-1} . Noting that the latter speed is about a 100 m a^{-1} higher than that measured by *Simmons*

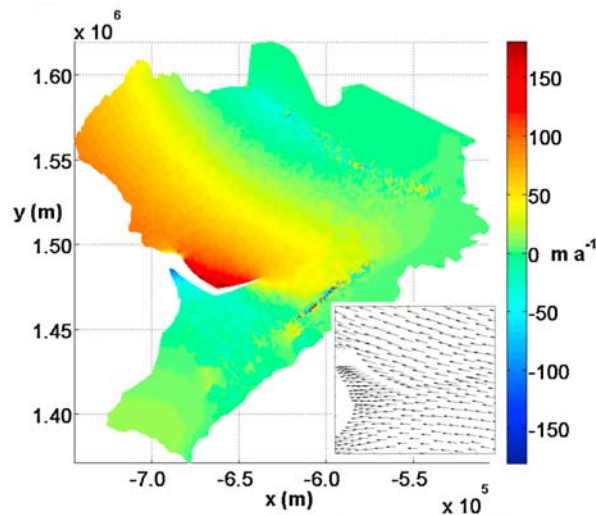


Figure 6. Speed change due to frontal rift propagation, obtained by subtracting the results of the simulation with an intact ice shelf front from those of the simulation of the open rift. The inset shows the resulting velocity vector field around the open frontal rift.

and Rouse [1984], and assuming that the weakness area of the transverse rifts and crevasses in the unnamed ice stream before the changes of the 1970s had the same general rheology of the stiffer surrounding area, we raise its flow parameter value to $1.3 \times 10^8 \text{ Pa s}^{1/3}$ (Figure 4e) which yields a better agreement of 787 m a^{-1} (Figure 5b). Thus, by making a simple modification to the rheology field inferred for the present-day BSW system, taking into account changes in the 1970s, we are able to reliably reproduce velocities observed during that period. This supports the hypothesis that the acceleration was caused by rheological changes in the ice mélange areas.

4.3. Enlargement of the Frontal Rift

[24] One of the main areas of weaker ice, as pointed out above, is the prominent rift extending from the ice shelf front through the ice mélange area to the interior (Figure 1). The presence here of extensive fracture revealed in our inferred rheology suggests that this could be a location where the frontal rift can widen and extend further into the ice shelf, perhaps acting as prelude to a future major calving event of the Stancomb-Wills Ice Tongue. The likelihood of rift widening here is raised by the findings of Leonard *et al.* [2008] that rifts at the front, being more exposed to warmer waters, are less likely to be filled with stabilizing mélange. This is also the area where ice shelf flow reaches its highest speed. We tested for the possible consequences on the flow regime of the BSW system by simulating a widening of the rift already visible in the radar image (Figure 1), tracing its possible future outline (Figure 6) and progression inward along the line of abrupt change discernible in the observed velocity field (Figure 2a). We ran the forward model using the inferred rheology with the enlarged rift and compared the resulting velocity magnitude field with that for the case of an intact ice shelf front. The result (Figure 6) clearly suggests that once the rift starts opening, the flow regime of

the ice shelf will be modified in a manner that induces further enlargement. Thus, the western part of Stancomb-Wills upstream from the rift will increase in speed by 70 to 160 m a^{-1} , while south of the rift the tendency is for the ice to slow down by about 30 m a^{-1} in places. Furthermore, Figure 6 shows that the flow north of the long southern rift will increase by up to 50 m a^{-1} , with little change on the southern side, which could result in that rift widening as well.

[25] The results of this simulation therefore point to the strong likelihood of further future widening and extension of the frontal and southern rifts.

4.4. Ice Shelf Stability

[26] The results presented above provide several indications to the current and future stability of the BSW system. Generally, the ice shelf is noticeably stiffer than the Larsen B Ice Shelf shortly before its disintegration [Khazendar *et al.*, 2007, Figure 2] and in comparison contains fewer zones of weakness, which here are mostly located at the front, near the margins of the domain along the lines of sharp velocity gradients as well as along the grounding line of Brunt Ice Shelf. This latter area is dominated by extensive fracturing of the ice, most likely caused by the steep surface slope, as it arrives at the grounding line and starts to float [Ardus, 1965; Thomas, 1973b]. Yet farther downstream the ice in our inferred rheology field (Figure 4a) appears to be more solid, implying that the open rifts and bottom crevasses must have gradually filled with marine ice, in addition to other mélange components, as they traveled toward the front in a process similar to that modeled by Khazendar and Jenkins [2003]. Also, the extensive fault between N9 and the rift southeast of First Chasm imprints the inferred rheology with a corresponding line of weakness relative to the surrounding ice, but not nearly as weak as the other main fracture zones in the system. This consolidation of previously fractured ice revealed here strongly supports the argument that areas of mélange including accreted marine ice play an important role in holding the disparate parts of an ice shelf together, therefore enhancing its stability.

[27] In addition, no major calving occurred after a fault traversed Brunt proper from its grounding line to the front which demonstrates the additional role of the McDonald Ice Rumples in holding that part of the ice shelf in place.

[28] The relatively high stiffness of the BSW system that we inferred here indicates that the ice shelf in its current configuration is unlikely to be prone to the type of rapid, extensive disintegration that occurred on Larsen B in 2002. On the other hand, our work shows that it could be vulnerable to other destabilizing factors, such as additional propagation of the frontal rift into the ice shelf. A recent analysis [British Antarctic Survey, 2005] emphasized the fact that the Stancomb-Wills Ice Tongue has been extending for the last 50 years and is currently at its most advanced state since 1915, and that its calving might represent a hazard to Halley Station if a calved section collides with Brunt proper. Our simulation shows that frontal rift propagation could become part of a positive feedback process, which could also enhance rifting elsewhere and destabilize the BSW system. Khazendar *et al.* [2007] showed the link that existed in the case of Larsen B between, on the one hand, major frontal retreat and, on the other, an accelerated

ice shelf flow and enhanced fracture. *Vieli et al.* [2007] found a similar link.

[29] Over the longer term, the highly heterogeneous structure of the ice shelf, and the role revealed here that marine ice could play as part of the mélange in keeping its mechanical integrity and shaping its flow regime also exposes a possible vulnerability. Both the rate of formation of frazil crystals [*Jenkins and Bombosch*, 1995; *Tison et al.*, 2001; *Khazendar and Jenkins*, 2003], and the structural integrity of marine ice layers that result from their accretion, are highly sensitive to the properties of ocean water [*Craven et al.*, 2005]. In particular, ice shelf basal melting rates are very sensitive to small changes in temperature. Thus, *Rignot and Jacobs* [2002] showed that a 1°C increase in oceanic thermal forcing can increase melting rates by up to 10 m a⁻¹, and *Holland et al.* [2008] found a quadratic relationship between total ice shelf basal melting and ocean warming. This, combined with the enhanced exposure of marine ice especially in its permeable layers, is important in explaining ice shelf flow changes on shorter time scales.

[30] Changes in ocean water properties can diminish the rate of frazil crystal accretion, increase melting and lower the mechanical competence of the already existing marine ice and, ultimately, the stability of the ice shelf. The narrowness of the continental shelf off Brunt and Stancomb-Wills makes their underlying ocean cavities more exposed to water masses from the Weddell Sea and any possible future changes in their properties or circulation patterns. In general, such interactions emphasize the strong link and interdependence between the evolution of ice shelves and that of the Southern Ocean at large.

5. Conclusions

[31] The methods and techniques employed in this work confirm the effectiveness of data assimilation in taking advantage of the increasingly available high-resolution satellite observations in the study of ice shelf processes. The results contribute to the study of the specific case of the Brunt/Stancomb-Wills Ice shelf, and the wider issue of mélange and marine ice in Antarctic ice shelves. We have inferred the flow parameter field of the Brunt/Stancomb-Wills system, which is valuable for improving forward modeling of its present and future flow regime; demonstrated the sensitivity of ice shelf flow to changes in the flow parameter; presented a plausible explanation for the observed ice shelf acceleration in the 1970s; and explored the potential risk it faces from rift enlargement or a change in the properties of the ice mélange areas. Our findings on Brunt give strong support to the general idea of ice mélange being able, at least partially, to fill ice shelf fracture, such as rifts and bottom crevasses, as well as larger expanses separating meteoric ice segments of an ice shelf and being an important factor in ice shelf stability.

[32] More generally, we have taken the first step in quantifying a difference in rheology between marine and meteoric ice outside of a laboratory setting by the use of remote sensing and numerical modeling methods. As marine ice forms the bulk of ice shelf thickness at many locations in Antarctica, allowing for its different stiffness is valuable for more accurate models of ice shelf flow and evolution. The simulations here present a strong demon-

stration of the role the changing properties of a marine ice body could have on the flow and stability of an ice shelf. This is more pertinent still given that marine ice can be highly porous in its lower layers, making its interaction with ocean water take place over a surface area that is much larger than would be the case at a nonporous ice shelf base, keeping its temperature closer to the freezing point and affecting its mechanical behavior. Importantly in the context of global climate change, with small changes in ocean water temperature known to result in large increases in ice shelf basal melting rates, the enhanced exposure of marine ice means that relatively small changes in the properties of ocean water in the subice shelf cavities could lead to rapid modifications in the flow of these ice shelves. This calls attention to the extent to which the vulnerability of many seemingly stable ice shelves could be underestimated.

[33] **Acknowledgments.** Part of this work was performed by the first author as a fellow of the NRC/Oak Ridge Associated Universities NASA Postdoctoral Program. He would like to thank A. Humbert, B. Kulesa, A. Luckman, K. Makinson, and K. Nicholls for informative discussions. We much appreciate the thorough and highly informative comments of O. Sergienko, two anonymous reviewers, and the Associate Editor. This work was performed at the Jet Propulsion Laboratory, California Institute of Technology, under contract with the National Aeronautics and Space Administration, with support from NASA's Cryospheric Sciences Program.

References

- Ardus, D. A. (1965), Morphology and regime of the Brunt Ice Shelf and the adjacent inland ice, 1960–61, *Br. Antarct. Surv. Bull.*, 5, 13–42.
- Beckmann, A., and R. Timmermann (2001), Circumpolar Influences on the Weddell Sea: Indication of an Antarctic Circumpolar Coastal Wave, *J. Clim.*, 14, 3785–3792, doi:10.1175/1520-0442(2001)014<3785:CIOTWS>2.0.CO;2.
- British Antarctic Survey (2005), Proposed construction and Operation of Halley VI Research Station, Brunt Ice Shelf, Antarctica, draft comprehensive environmental evaluation (CEE), Cambridge, U. K.
- British Antarctic Survey (2007), Proposed construction and Operation of Halley VI Research Station, and demolition and removal of Halley V Research Station, Brunt Ice Shelf, Antarctica, final comprehensive environmental evaluation, Cambridge, U. K.
- Carsey, F. D. (1980), Microwave observations of the Weddell Polynya, *Mon. Weather Rev.*, 108, 2032–2044, doi:10.1175/1520-0493(1980)108<2032:MOOTWP>2.0.CO;2.
- Craven, M., I. Allison, R. Brand, A. Elcheikh, J. Hunter, M. Hemer, and S. Donoghue (2004), Initial borehole results from the Amery Ice Shelf hot water drilling project, *Ann. Glaciol.*, 39, 531–539, doi:10.3189/172756404781814311.
- Craven, M., F. Carsey, A. Behar, J. Matthews, R. Brand, A. Elcheikh, S. Hall, and A. Treverrow (2005), Borehole imagery of meteoric and marine ice layers in the Amery Ice Shelf, *J. Glaciol.*, 51(172), 75–84, doi:10.3189/172756505781829511.
- DiMarzio, J., A. Brenner, R. Schutz, C. A. Shuman, and H. J. Zwally (2007), GLAS/ICESat 500 m laser altimetry digital elevation model of Antarctica, digital media, Natl. Snow and Ice Data Cent., Boulder, Colo.
- Doake, C. (2000), Recent glaciological investigations on Brunt Ice Shelf, in *14th International Workshop of the Filchner-Ronne Ice Shelf Programme held at Madingley Hall, Cambridge, U.K. on 15th–16th June 1999*, edited by H. Oerter, *FRISP Rep.* 13, pp. 13–18, Alfred-Wegener-Inst. for Polar and Mar. Res., Bremerhaven, Germany.
- Doake, C. S. M., and D. G. Vaughan (1991), Rapid disintegration of the Wordie Ice Shelf in response to atmospheric warming, *Nature*, 350, 328–330, doi:10.1038/350328a0.
- Doake, C. S. M., H. F. J. Corr, K. W. Nicholls, A. Gaffikin, A. Jenkins, W. I. Bertiger, and M. A. King (2002), Tide-induced lateral movement of Brunt Ice Shelf, Antarctica, *Geophys. Res. Lett.*, 29(8), 1226, doi:10.1029/2001GL014606.
- Eicken, H., H. Oerter, H. Miller, W. Graf, and J. Kipfstuhl (1994), Textural characteristics and impurity content of meteoric and marine ice in the Ronne Ice Shelf, Antarctica, *J. Glaciol.*, 40, 386–398.
- Engelhardt, H., and J. Determann (1987), Borehole evidence for a thick layer of basal ice in the central Ronne Ice Shelf, *Nature*, 327, 318–319, doi:10.1038/327318a0.

- Fofonoff, N. P., and R. C. Millard (1983), Algorithms for computation of fundamental properties of seawater, *UNESCO Tech. Pap. Mar. Sci.* 44, UNESCO, Paris.
- Fricker, H. A., S. Popov, I. Allison, and N. Young (2001), Distribution of marine ice beneath the Amery Ice Shelf, *Geophys. Res. Lett.*, 28(11), 2241–2244, doi:10.1029/2000GL012461.
- Gordon, A. L. (1982), Weddell Deep Water variability, *J. Mar. Res.*, 40, 199–217.
- Haran, T., J. Bohlander, T. Scambos, and M. Fahnestock (Compilers) (2005), MODIS mosaic of Antarctica (MOA) image map, digital media, Natl. Snow and Ice Data Cent., Boulder, Colo.
- Hayes, K. (2005), The Brunt Ice Shelf: Calving risks and ice shelf velocity, *Geophys. Res. Abstr.*, 7, 7.
- Helsen, M. M., M. R. van den Broeke, R. S. W. van de Wal, W. J. van de Berg, E. van Meijgaard, C. H. Davis, Y. Li, and I. Goodwin (2008), Elevation changes in Antarctica mainly determined by accumulation variability, *Science*, 320, 1626–1629, doi:10.1126/science.1153894.
- Holland, D. M. (2001), Explaining the Weddell Polynya—a Large Ocean Eddy Shed at Maud Rise, *Science*, 292, 1697–1700, doi:10.1126/science.1059322.
- Holland, P. R., A. Jenkins, and D. M. Holland (2008), The response of ice-shelf basal melting to variation in ocean temperature, *J. Clim.*, 21, 2558–2572, doi:10.1175/2007JCLI1909.1.
- Hulbe, C. L., R. Johnston, I. Joughin, and T. Scambos (2005), Marine ice modification of fringing ice shelf flow, *Arct. Antarct. Alp. Res.*, 37(3), 323–330, doi:10.1657/1523-0430(2005)037[0323:MIMOFI]2.0.CO;2.
- Humbert, A., and H. D. Pritchard (2006), Numerical simulations of the ice flow dynamics of the Brunt Ice Shelf–Stancomb Wills Ice Tongue System, in *19th International Workshop of the Forum for Research into Ice Shelf Processes held at Madingley Hall, Cambridge, U.K. on 21th–22th June 2006*, edited by L. Smedsrud, *FRISP Rep. 17*, pp. 1–13, Bjerknes Cent. for Clim. Res., Bergen, Norway.
- Jenkins, A., and A. Bomboch (1995), Modeling the effects of frazil ice crystals on the dynamics and thermodynamics of ice shelf water plumes, *J. Geophys. Res.*, 100, 6967–6981, doi:10.1029/94JC03227.
- Khazendar, A., and A. Jenkins (2003), A model of marine ice formation within Antarctic ice shelf rifts, *J. Geophys. Res.*, 108(C7), 3235, doi:10.1029/2002JC001673.
- Khazendar, A., J. L. Tison, B. Stenni, M. Dini, and A. Bondesan (2001), Significant marine ice accumulation in the ablation zone beneath an Antarctic ice shelf, *J. Glaciol.*, 47, 359–368, doi:10.3189/172756501781832160.
- Khazendar, A., E. Rignot, and E. Larour (2007), Larsen B Ice Shelf rheology preceding its disintegration inferred by a control method, *Geophys. Res. Lett.*, 34, L19503, doi:10.1029/2007GL030980.
- Lange, M. A., and H. Kohnen (1985), Ice front fluctuations in the eastern and southern Weddell Sea, *Ann. Glaciol.*, 6, 187–191.
- Larour, E., E. Rignot, and D. Aubry (2004), Modelling of rift propagation on Ronne Ice Shelf, Antarctica, and sensitivity to climate change, *Geophys. Res. Lett.*, 31, L16404, doi:10.1029/2004GL020077.
- Larour, E., E. Rignot, I. Joughin, and D. Aubry (2005), Rheology of the Ronne Ice Shelf, Antarctica, inferred from satellite radar interferometry data using an inverse control method, *Geophys. Res. Lett.*, 32, L05503, doi:10.1029/2004GL021693.
- Leonard, K. C., L.-B. Tremblay, D. R. MacAyeal, and S. S. Jacobs (2008), Interactions of wind-transported snow with a rift in the Ross Ice Shelf, Antarctica, *Geophys. Res. Lett.*, 35, L05501, doi:10.1029/2007GL033005.
- Liu, H., L. Wang, and K. C. Jezek (2006), Spatiotemporal variations of snowmelt in Antarctica derived from satellite scanning multichannel microwave radiometer and Special Sensor Microwave Imager data (1978–2004), *J. Geophys. Res.*, 111, F01003, doi:10.1029/2005JF000318.
- MacAyeal, D. (1989), Large-scale ice flow over a viscous basal sediment: Theory and application to Ice Stream B, Antarctica, *J. Geophys. Res.*, 94(B4), 4071–4087, doi:10.1029/JB094iB04p04071.
- MacAyeal, D. (1992), The basal stress distribution of Ice Stream E, Antarctica, inferred by control methods, *J. Geophys. Res.*, 97(B1), 595–603, doi:10.1029/91JB02454.
- MacAyeal, D. R., E. Rignot, and C. L. Hulbe (1998), Ice-shelf dynamics near the front of the Filchner-Ronne Ice Shelf, Antarctica, revealed by SAR interferometry: Model/interferogram comparison, *J. Glaciol.*, 44, 419–428.
- Moore, J. C., A. P. Reid, and J. Kipfstuhl (1994), Microstructure and electrical properties of marine ice and its relationship to meteoric ice and sea ice, *J. Geophys. Res.*, 99(C3), 5171–5180, doi:10.1029/93JC02832.
- Morgan, V. I. (1972), Oxygen isotope evidence for bottom freezing on the Amery Ice Shelf, *Nature*, 238, 393–394, doi:10.1038/238393a0.
- Oerter, H., H. Eicken, J. Kipfstuhl, H. Miller, and W. Graf (1994), Comparison between ice core B13 and B15, in *8th International Workshop of the Filchner-Ronne Ice Shelf Programme held at Madingley Hall, Cambridge, U.K. on 10th–11th June 1993: Filchner-Ronne Ice Shelf Programme*, edited by H. Oerter, *FRISP Rep. 7*, pp. 29–36, Alfred-Wegener-Institut for Polar and Mar. Res., Bremerhaven, Germany.
- Orheim, O. (1986), Flow and thickness of Riiser-Larsenisen, Antarctica, *Nor. Polarinst. Skr.*, 187, 5–22.
- Paterson, W. S. B. (1994), *The Physics of Glaciers*, 4th ed., Elsevier, New York.
- Renfrew, I. A., and P. S. Anderson (2002), The surface climatology of an ordinary katabatic wind regime in Coats Land, Antarctica, *Tellus, Ser. A*, 54, 463–484.
- Rignot, E. (2002), Mass balance of East Antarctic glaciers and ice shelves from satellite data, *Ann. Glaciol.*, 34, 217–227, doi:10.3189/172756402781817419.
- Rignot, E., and S. S. Jacobs (2002), Rapid bottom melting widespread near Antarctic Ice Sheet grounding lines, *Science*, 296, 2020–2023, doi:10.1126/science.1070942.
- Rignot, E., and D. R. MacAyeal (1998), Ice-shelf dynamics near the front of the Filchner-Ronne Ice Shelf, Antarctica, revealed by SAR interferometry, *J. Glaciol.*, 44, 405–418.
- Rignot, E., G. Casassa, P. Gogineni, W. Krabill, A. Rivera, and R. Thomas (2004), Accelerated ice discharge from the Antarctic Peninsula following the collapse of Larsen B ice shelf, *Geophys. Res. Lett.*, 31, L18401, doi:10.1029/2004GL020697.
- Rist, M. A., P. R. Sammonds, H. Oerter, and C. S. M. Doake (2002), Fracture of Antarctic shelf ice, *J. Geophys. Res.*, 107(B1), 2002, doi:10.1029/2000JB000058.
- Robertson, R., M. Visbeck, A. L. Gordon, and E. Fahrbach (2002), Long-term temperature trends in the deep waters of the Weddell Sea, *Deep Sea Res., Part II*, 49, 4791–4806, doi:10.1016/S0967-0645(02)00159-5.
- Rommelaere, V., and D. MacAyeal (1997), Large-scale rheology of the Ross Ice Shelf, Antarctica, computed by a control method, *Ann. Glaciol.*, 24, 43–48.
- Scambos, T. A., J. A. Bohlander, C. A. Shuman, and P. Skvarca (2004), Glacier acceleration and thinning after ice shelf collapse in the Larsen B embayment, Antarctica, *Geophys. Res. Lett.*, 31, L18402, doi:10.1029/2004GL020670.
- Simmons, D. A. (1986), Flow of the Brunt Ice Shelf, Antarctica, derived from Landsat images, 1974–85, *J. Glaciol.*, 32, 252–254.
- Simmons, D. A., and J. R. Rouse (1984), Accelerating flow of the Brunt Ice Shelf, Antarctica, *J. Glaciol.*, 30, 377–380.
- Stephenson, S. N., and H. J. Zwally (1989), Ice-shelf topography and structure determined using satellite-radar altimetry and Landsat imagery, *Ann. Glaciol.*, 12, 161–164.
- Thoma, M., K. Grosfeld, and M. A. Lange (2006), Impact of the Eastern Weddell Ice Shelves on water masses in the eastern Weddell Sea, *J. Geophys. Res.*, 111, C12010, doi:10.1029/2005JC003212.
- Thomas, R. H. (1973a), The creep of ice shelves: Theory, *J. Glaciol.*, 12, 45–53.
- Thomas, R. (1973b), The dynamics of the Brunt Ice Shelf, Coats Land, Antarctica, *Sci. Rep. 79*, Br. Antarct. Surv., Cambridge, U. K.
- Thomas, R. (2007), Tide induced perturbations of glacier velocities, *Global Planet. Change*, 59, 217–224, doi:10.1016/j.gloplacha.2006.11.017.
- Tison, J.-L., A. Khazendar, and E. Roulin (2001), A two-phase approach to the simulation of the combined isotope/salinity signal of marine ice, *J. Geophys. Res.*, 106(C12), 31,387–31,402, doi:10.1029/2000JC000207.
- van den Broeke, M. R. (2000), The semiannual oscillation and Antarctic climate, part 3: The role of near-surface wind speed and cloudiness, *Int. J. Climatol.*, 20, 117–130, doi:10.1002/(SICI)1097-0088(200002)20:2<117::AID-JOC481>3.0.CO;2-B.
- van den Broeke, M. R. (2006), Towards quantifying the contribution of the Antarctic ice sheet to global sea level change, *J. Phys. IV*, 139, 173–185, doi:10.1051/jp4:2006139013.
- van den Broeke, M. R. (2008), Depth and density of the Antarctic firn layer, *Arct. Antarct. Alp. Res.*, 40(2), 432–438, doi:10.1657/1523-0430(07-021)[BROEKE]2.0.CO;2.
- Vieli, A., A. J. Payne, Z. Du, and A. Shepherd (2006), Numerical modeling and data assimilation of the Larsen B ice shelf, Antarctic Peninsula, *Philos. Trans. R. Soc. S. Afr.*, 364, 1815–1839, doi:10.1098/rsta.2006.1800.
- Vieli, A., A. J. Payne, A. Shepherd, and Z. Du (2007), Causes of pre-collapse changes of the Larsen B ice shelf: Numerical modelling and assimilation of satellite observations, *Earth Planet. Sci. Lett.*, 259, 297–306, doi:10.1016/j.epsl.2007.04.050.

A. Khazendar and E. Larour, Jet Propulsion Laboratory, California Institute of Technology, Mail Stop 300-319, 4800 Oak Grove Drive, Pasadena, CA 91109, USA. (ala.khazendar@jpl.nasa.gov)

E. Rignot, Earth System Science, University of California, Croul Hall, Irvine, CA 92697, USA.